



High heat flux simulation experiments with improved electron beam diagnostics

J. Linke^{a,*}, H. Bolt^b, R. Duwe^a, W. Kühnlein^a, A. Lodato^a, M. Rödiger^a,
K. Schöpflin^a, B. Wiechers^a

^a *Forschungszentrum Jülich, EURATOM Association, D-52425 Jülich, Germany*

^b *Max-Planck-Institut für Plasmaphysik, Boltzmannstraße 2, D-85748 Garching, Germany*

Abstract

Plasma facing materials such as beryllium, carbon or tungsten are subjected to intense heat loads during off-normal plasma operation. To simulate these events, electron beam experiments are performed routinely to investigate the thermomechanical performance of the materials. In these tests, main emphasis has been laid on the material damage such as melting, cracking, and degradation of the materials' properties. On the other hand, severe thermal loads are also associated with the release of particles from the loaded surface (metallic droplets or carbon dust) which might contaminate the plasma in future fusion devices. To investigate these phenomena in high heat flux simulation tests, extensive diagnostics are required to evaluate the actual material loading and to characterize the resulting material damage. Among these are measurements of the electrical current through the test coupons and high-speed IR pyrometry. © 2000 Elsevier Science B.V. All rights reserved.

1. Introduction

To investigate the thermal response of plasma facing materials and components under tokamak relevant heat loads, electron beam or ion beam experiments are being used. These above-mentioned techniques are frequently applied for high heat flux tests simulating the normal operation conditions of divertor, limiter or first wall components (quasi-stationary loading). These tests also include transient heat loads during plasma instabilities such as vertical displacement events (VDE) ($t_{\text{pulse}} \approx 0.1\text{--}1$ s). The simulation of incidents on a shorter time scale such as plasma disruptions ($t_{\text{pulse}} \approx 1$ ms) have been investigated primarily in plasma accelerators; these tests allow complex loading conditions including vapor shielding or magnetic field effects. To perform material screening and to investigate the thermally induced material damage (melting, evaporation,

crack formation, etc.), electron beams have been used effectively as well.

For any type of high heat flux simulation experiment it is essential to characterize the incident beam energy and the fraction which is absorbed by the specimen surface. During the transient phase, a non-negligible fraction may be absorbed by the ablation vapor or will be reflected; this amount depends strongly on the loading parameters and on the nature of the test material. To quantify the resulting material damage, a well-diagnosed test equipment is indispensable. Beside comprehensive measurements of the electrical current in the test samples, the resulting surface temperature has been recorded by a high-speed IR pyrometer; additional diagnostics include calorimetry, weight loss measurements, profilometry and different metallographic and optical procedures.

2. High heat flux simulation experiments

The major fraction of experiments described in this paper has been performed in the electron beam test facility JUDITH [1]. A focused electron beam with typical

* Corresponding author. Tel.: +49-2461 61 3230; fax: +49-2461 61 3687.

E-mail address: j.linke@fz-juelich.de (J. Linke).

energies of 120 keV is scanned across the surface of the test coupon to guarantee a rather homogeneous heat load profile; typical scanning frequencies are in the order of 40–60 kHz. The ratio of the frequencies in x - and y -directions has to be selected carefully to avoid hot spots or other non-uniform load patterns (Lissajous-patterns). Depending on the applied heat fluxes loaded surface areas of typically $3 \times 3 \text{ mm}^2$ up to $15 \times 15 \text{ mm}^2$ have been selected; the former primarily for the simulation of disruption heat loads on refractory metals with high reflection coefficients (pulse duration $\sim 5 \text{ ms}$); the latter for the imitation of vertical displacement events on actively cooled modules with carbon or beryllium armor at pulse durations of 1 s [2].

Depending on the selected materials, part of the incident electrons are reflected from the sample surface and do not contribute to surface heating. This fraction is relatively low for beryllium or carbon-based materials (typically, a few % for electron energies of 120 keV; however, for tungsten this factor increases to $\sim 50\%$). To allow for energy losses due to reflected electrons the absorbed current during electron beam loading has been monitored using an electrically isolated test coupon, which is grounded by a resistor of 100Ω . The voltage drop at this resistor determines the current. At elevated surface temperatures beside electron reflection a second phenomenon, namely thermionic emission is becoming essential. To control this current as well, a probe consisting of an isolated copper plate positioned at $\sim 50 \text{ mm}$ from the heated surface has been installed in the vacuum chamber of the test facility. This method cannot provide quantitative data, since only a relatively small fraction of the reflected or thermally emitted electrons are trapped. To obtain quantitative results, an isolated tube encircling the incident electron beam has been used; however, this method does not allow other diagnostics (e.g. pyrometers) since the heated surface of the plasma facing material is optically shielded [3].

To determine the resulting surface temperature during electron beam loading, a fast pyrometer has been developed by ZFK–HZ at Forschungszentrum Jülich (Fig. 1). The optical sensor consists of a silicon photodiode with an integrated preamplifier. A surface area of $\sim 2 \text{ mm}$ in diameter is projected using a 75 mm lens. To facilitate the adjustment of the pyrometer system (which is positioned outside the vacuum chamber), a laser target light is projected on the surface of the test coupon using a beam splitter. The response time of this system is below $0.5 \mu\text{s}$. This has been calibrated with the input pulse from an infrared diode (cf. Fig. 2). Hence, the system is fast enough to perform surface temperature measurements during disruption simulation experiments. A careful calibration of the measuring system has been performed using fine grain graphite as a reference material. This material has a well-defined emissivity ($\varepsilon = 0.8$) up to high temperatures of $\sim 3000 \text{ K}$. Due to

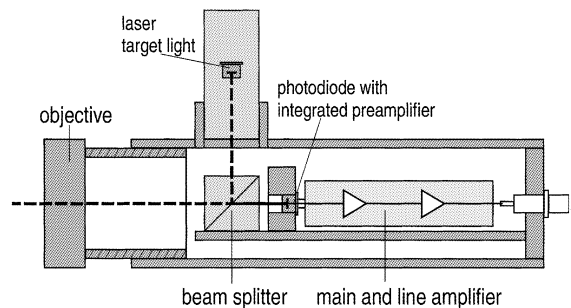


Fig. 1. Fast pyrometer for surface temperature measurement during transient heat loads.

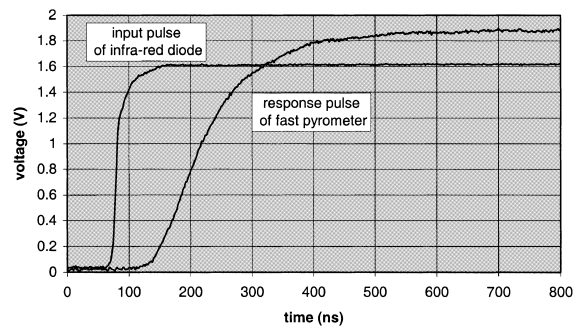


Fig. 2. Response of the fast pyrometer to an infrared signal.

oxidation or phase transitions exact surface temperature measurements on metallic test coupons are much more complex.

3. Results

Test coupons made from different plasma facing materials (beryllium, tungsten alloys, and carbon-based materials) have been exposed to intense electron beam pulses to simulate the thermal load during plasma disruptions. In these tests, absorbed energy densities for up to $\sim 15 \text{ MJ m}^{-2}$ have been applied; the pulse durations were typically 5 ms. Under these conditions all metallic samples showed severe melting; in addition, the formation of thermal shock-induced cracks (in the recrystallized material, for some PFMs even in the bulk) has been detected. Even in refractory metals such as tungsten, melting of the electron beam exposed surfaces was typically observed. Fig. 3 shows the surface morphology of a plasma sprayed tungsten coating (1 mm thickness) on a copper substrate. At an incident energy density of 11.5 MJ m^{-2} , the loaded surface shows severe melting; in addition a dense crack pattern throughout the loaded surface is detectable. The whole surface is covered with globular objects of resolidified tungsten (typical

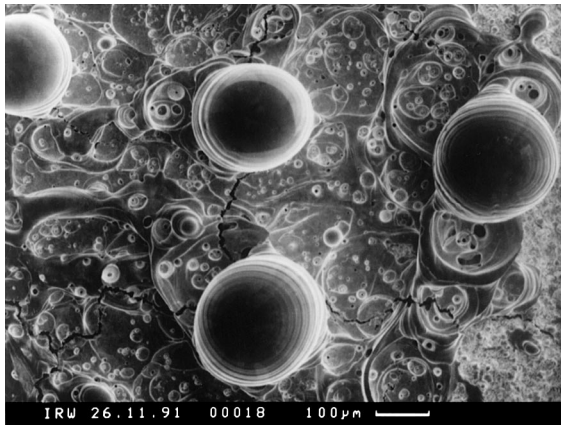


Fig. 3. Surface of plasma sprayed tungsten on a copper substrate after thermal shock loading in the electron beam ($E_{\text{inc}} = 11.5 \text{ MJ m}^{-2}$, $t_{\text{pulse}} = 2 \text{ ms}$, five shots).

diameter of the globular particles is $200 \mu\text{m}$). Under realistic tokamak conditions in the presence of additional magnetic forces and plasma pressure these objects can easily contaminate the plasma boundary layer. This effect is even worse for materials with a low melting point such as beryllium.

In Fig. 4, the absorbed current during short-term electron beam bombardment has been measured for three different metals. Identical electron beam pulses of 5 ms duration have been applied to aluminum, beryllium, and stainless steel on an area of $4 \times 4 \text{ mm}^2$. The acceleration voltage was 120 kV; the incident beam current was 200 mA. For aluminum an absorbed current of $\sim 170 \text{ mA}$ was measured; this current remains constant up to the end of the electron beam pulse. Hence, the current of backscattered electrons is in the order of 30 mA, i.e. $\sim 15\%$. Materials with a higher melting

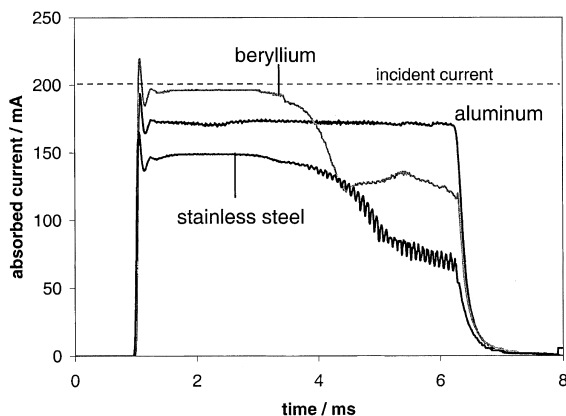


Fig. 4. Absorbed current during electron beam loading of beryllium, aluminum, and stainless steel ($I_{\text{inc}} = 200 \text{ mA}$, $E = 120 \text{ keV}$, $t_{\text{pulse}} = 5 \text{ ms}$, area = $4 \times 4 \text{ mm}^2$).

temperature show a different behavior: In the case of beryllium, the fraction of backscattered electrons is due to the low- Z nature of this material significantly smaller (below 5%). However, the absorbed current does not remain constant; after $\sim 2 \text{ ms}$ the absorbed current drops continuously to values of 120–130 mA. This drop is mainly caused by thermionic emission of the heated surface. For all metals (Be, Al, SS) melting occurs within the first two milliseconds of the electron beam pulse. Due to the relatively large penetration depth of 120 keV electrons in a low- Z material ($\sim 150 \mu\text{m}$ in beryllium), the formation of a melt layer is not restricted to the outer surface alone; according to model calculations using the finite element code ABAQUS a relatively thick layer will undergo phase transition. Now intense electron beam-induced convection [4] will take place in the melt layer; the temperature will further increase until an equilibrium of beam heating and evaporation cooling is reached. For beryllium this temperature has been calculated to be about 2000°C [5]. At this temperature, the thermally induced electron emission of a metallic surface (electronic work function of Be = 3.92 eV) is $\sim 5 \text{ mA mm}^{-2}$ [6]. Hence, the electron beam heated beam spot ($4 \times 4 \text{ mm}^2$) will emit an electrical current of about 80 mA, which corresponds to the observed current drop. Similar effects might cause the current drop in stainless steel. Aluminum with a significantly lower melting point ($T_m = 660^\circ\text{C}$) will not reach any temperature where thermionic emission is becoming essential.

The drop in the absorbed current, both for beryllium and stainless steel does not affect the heat transfer into the test coupon; from an energy viewpoint, the energy of the thermally emitted electrons can be neglected compared to the incident energy of 120 keV per electron.

A similar behavior has been observed for graphite. Test coupons made from an isotropic fine-grain graphite EK98 have been exposed to beam pulses of 350 mA, cf. Fig. 5. As long as the loaded surface remains at temperatures $\sim 1500^\circ\text{C}$, i.e. during the first millisecond of

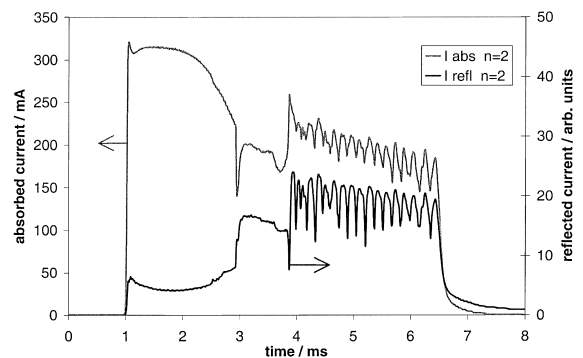


Fig. 5. Absorbed and reflected current during electron beam loading of a 3-D CFC material (Dunlop Concept 1, $E_{\text{inc}} = 7.68 \text{ MJ m}^{-2}$, $t_{\text{pulse}} = 5 \text{ ms}$, second shot, area = $5 \times 5 \text{ mm}^2$).

the electron beam pulse, the absorbed current stabilizes at about 315 mA, which corresponds to a backscattered fraction of less than 10%. However, a rapid surface heating results in a sharp decrease of the absorbed current due to thermionic emission. Simultaneously the reflected current increases. After 2 ms, both the absorbed and the reflected currents are coupled. Obviously, a dense vapor layer has been formed due to the intense evaporation of carbon; this vapor is ionized and the resulting plasma will bridge the two electrodes, i.e. the test sample and the isolated copper probe. The spiking with a frequency of ~ 5 kHz might be due to plasma oscillations.

In a previous paper, it has been reported that intense thermal loads on carbon-based materials result in the formation of dust particles [7]. This particle emission is a consequence of the brittle destruction of graphite or CFCs. During repeated electron beam pulses on the polished graphite surface the intensity of particle emission decreases significantly. After 5–10 pulses, a steady-state erosion is detectable, i.e. a conditioning of the surface occurs. In a polished test coupon, some of the surface grains are intersected and can be removed easily from the graphite matrix. In addition, the binder phase, which provided the thermal contact between individual grains, is eroded preferentially during intense thermal loads. As a consequence, the formation of hot spots due to loosely bound carbon particles is more likely in a polished test coupon. The thermionic emission from an electron beam heated graphite surface is strongly enhanced by hot spots; hence, the absorbed current in a polished surface will be less compared to a ‘conditioned’ surface. This fact can be clearly seen in Figs. 5 and 6. Fig. 5 represents the second electron pulse ($n = 2$) on a fresh polished surface; Fig. 6 shows the same sample after five identical electron beam shots ($n = 5$). In the latter case, the thermionic emission is less intense. The surface temperatures measured with the high-speed pyrometer for both experiments are plotted in Fig. 7. In

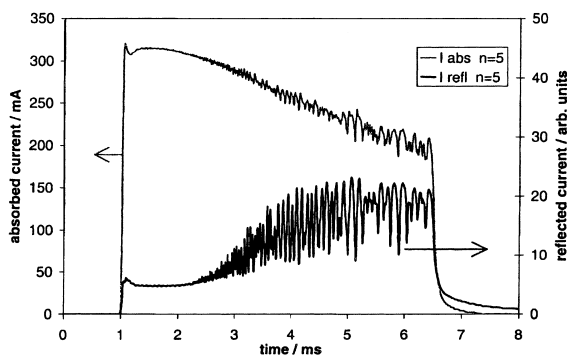


Fig. 6. Absorbed and reflected current during repeated electron beam loading of a 3-D CFC material (Dunlop Concept 1, $E_{inc} = 7.68 \text{ MJ m}^{-2}$, $t_{pulse} = 5 \text{ ms}$, fifth shot, area = $5 \times 5 \text{ mm}^2$).

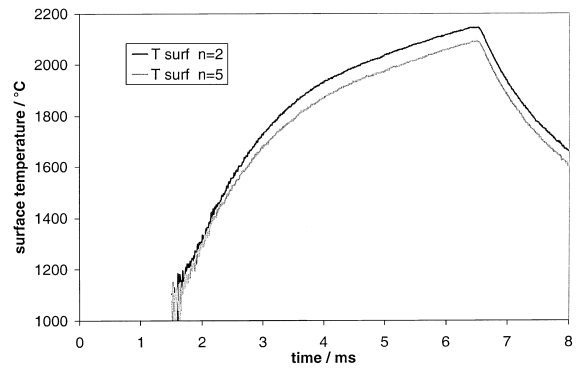


Fig. 7. Surface temperature during electron beam loading experiments in Figs. 5 and 6.

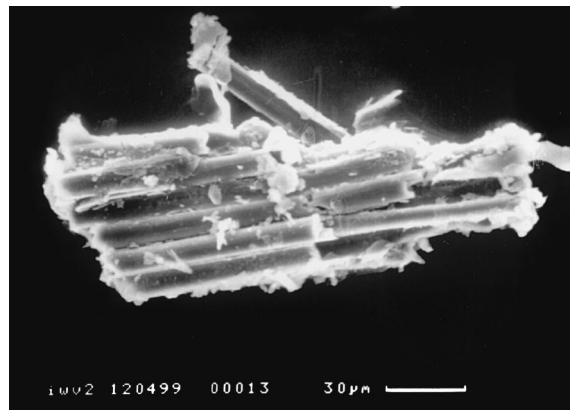


Fig. 8. Carbon fragments generated during electron beam loading of a 3-D CFC material (SEPCarb NB31, $U_B = 120 \text{ kV}$, $I_B = 30 \text{ mA}$, $t_{pulse} = 0.2 \text{ s}$).

both cases, maximum temperatures slightly above 2000°C have been measured; these data are integrated values for a spot size of $\sim 2 \text{ mm}$ in diameter. The higher fraction of hot spots in the second electron beam pulse results in an apparently higher surface temperature. It should be noted that the measured surface temperature increases monotonously and is not affected by the strong decrease in the absorbed beam current (cf. Fig. 7).

The emission of dust particles from heated graphite surfaces may have a significant impact on the plasma performance and safety issues in future thermonuclear tokamak facilities. Speculations that multidirectional carbon fiber composites with superior thermal and mechanical properties might not be affected by brittle destruction processes could not be confirmed up to now [8]. Electron beam load tests on a 3-D CFC material (SEPCarb NB31) show a similar amount of carbon dust which additionally contains a relatively high fraction of carbon fiber segments – individual fibers as well as small fiber clusters, cf. Fig. 8.

4. Conclusions

The behavior of different plasma facing materials under high transient heat loads has been investigated in electron beam simulation experiments. To quantify the incident electron beam pulse and to characterize the thermal response of the test specimens, improved diagnostics have been utilized. Among these are a fast pyrometer with a thermal response time $<0.5 \mu\text{s}$ and probes for the measurement of absorbed and reflected currents. During short electron beam pulses with power densities in the order of $\geq 1 \text{ GW m}^{-2}$ metallic test coupons will undergo melting within milliseconds. Further heating of the melt layer will result in a reduction of the absorbed current due to thermionic emission; nevertheless, the energy of the incident electrons is deposited in the melt layer. For carbon-based materials the absorbed current strongly depends on the morphology of the material surface. On polished surfaces hotspots are formed due to loosely bound carbon grains and due to brittle destruction. Part of these grains are released in the form of dust.

The formation of particles during intense heat loads is becoming essential both for metals and carbon-based materials. Recrystallized globular objects have been detected even on refractory metals (e.g. tungsten); carbon based materials form dust particles with diameters

of up to $100 \mu\text{m}$. In CFC materials even fiber segments or clusters of fibers are created.

References

- [1] M. Rödiger, M. Akiba, P. Chappuis, R. Duwe, M. Febvre, A. Gervash, J. Linke, N. Litunovski, S. Suzuki, D.L. Youchison, in: Proceedings of the Fifth International Symposium on Fusion Nuclear Technology, Rome, 19–24 September 1999.
- [2] M. Merola, M. Rödiger, J. Linke, R. Duwe, G. Vieider, *J. Nucl. Mater.* 258–263 (1998) 653.
- [3] A. Lodato, M. Rödiger, R. Duwe, H. Derz, J. Linke, R. Castro, A. Gervash, in: Proceedings of the Fifth International Symposium on Fusion Nuclear Technology, Rome, 19–24 September 1999.
- [4] P. Schiller, F. Brossa, M. Cambini, D. Quataert, G. Rigon, *Fus. Eng. Des.* 6 (1988) 131.
- [5] A. Schuster, J. Linke, M. Rödiger, H. Nickel, Ber. Forschungszentrums Jülich, 3437, ISSN 0944-2952, 1997.
- [6] M. von Ardenne, Tabellen zur Angewandten Physik, Deutscher Verlag der Wissenschaften, Berlin, 1962, p. 68ff.
- [7] J. Linke, R. Duwe, A. Gervash, R.H. Qian, M. Rödiger, A. Schuster, *J. Nucl. Mater.* 258–263 (1998) 634.
- [8] J. Linke, H. Bolt, P. Chappuis, H.J. Penkalla, M. Scheerer, K. Schöpflin, in: Proceedings of the Fifth International Symposium on Fusion Nuclear Technology, Rome, 19–24 September 1999.